Correlation Analysis of Instantaneous Mutual Information in 2×2 MIMO Systems

Shuangquan Wang, Ali Abdi

Center for Wireless Communications and Signal Processing Research
Department of Electrical and Computer Engineering
New Jersey Institute of Technology, Newark, New Jersey 07102
Email: sw27@njit.edu; ali.abdi@njit.edu

***Abstract*— In this paper, the second-order statistics such as the autocorrelation function and correlation coefficient of the instantaneous mutual information (IMI) are studied, in 2×2 multiple-input multiple-output (MIMO) time-varying Rayleigh flat fading channels, assuming general *non-isotropic* scattering environments. Exact closed-form expressions are derived, as well as asymptotic approximations in low- and high-SNR regimes. Monte Carlo simulations are provided to verify the accuracy of those derived analytical results.**

I. Introduction

The increasing demand for wireless communication over time-varying channels has motivated further investigation of the channel dynamics and their statistical behavior. There are numerous studies on the temporal correlations of a variety of terrestrial [1]–[4] and satellite channels [5].

For such important quantity as the *instantaneous mutual information* (IMI), however, only the mean value, which is the ergodic capacity, has received much attention as well as the outage probability [6][7]. Clearly, ergodic capacity and outage probability do not show the dynamic temporal behavior, such as correlations, of IMI in time-varying fading channels.

The IMI feedback is used for the rate scheduling in multi-user communication environments to increase the system throughput [8], where only the perfect feedback is considered. However, it is hard to obtain the perfect feedback in practice, and generally the feedbacked IMI is outdated. In this case, the correlation of IMI can be used to analyze the scheduling performance with outdated IMI feedbacks. Moreover, the correlation can also be used to improve the rate scheduling algorithm by exploring the correlation of IMI.

To the best of our knowledge, correlation analysis of IMI in single-input single-output (SISO) systems were reported in [9]. For MIMO systems, only some simulation results regarding correlation analysis are given in [10], without analytical results, and in [11], lower and upper bounds on the correlation coefficient in the high signal-to-noise ratio (SNR) regime, as well as some approximations, are derived without exact results.

In this paper, the second-order statistics such as the autocorrelation function and correlation coefficient of IMI are studied in 2×2 MIMO time-varying Rayleigh flat fading channels, where all the subchannels[1] are independent and identically distributed (i.i.d.) with the same temporal correlation coefficient, considering general *non-isotropic* scattering propagation environments. Closed-form expressions and simple approximations are derived for the autocorrelation function (ACF) and correlation coefficients of MIMO IMI. Monte Carlo simulations are provided to verify the accuracy of our closed-form expressions and approximate results.

Notation: † is reserved for matrix Hermitian, * for complex conjugate, $\jmath$ for $\sqrt{-1}$, $\mathbb{E}[\cdot]$ for mathematical expectation, $\mathbf{I}_m$ for the $m \times m$ identity matrix, $\ln(\cdot)$ for the natural logarithm, $\|\cdot\|_F$ for the Frobenius norm, $\Re[\cdot]$ and $\Im[\cdot]$ for the real and imaginary parts of a complex number, respectively, and $f^2(x)$ for $[f(x)]^2$.

The rest of this paper is organized as follows. Sec. II introduces the channel model and the IMI random process in multiple-input multiple-output (MIMO) systems, as well as angle-of-arrival (AoA) models. Sec. III is devoted to the derivation of ACF and correlation coefficient of IMI in 2×2 MIMO channels, as well as their low- and high-SNR asymptotic approximations. Numerical results are presented in Sec. IV, and concluding remarks are given in Sec. V.

II. Channel Model and MIMO IMI

For simplicity, only 2×2 MIMO time-varying Rayleigh flat fading channels are considered in this paper, and we assume all 4 suchannels, $\{h_{mn}(t)\}_{(m=1,n=1)}^{(2,2)}$ are i.i.d., with the same temporal correlation coefficient, i.e.,

$$\mathbb{E}[h_{mn}(t)h_{pq}^\star(t-\tau)] = \delta_{m,p}\delta_{n,q}\rho_h(\tau), \tag{1}$$

where the Kronecker symbol $\delta_{m,p}$ is 1 or 0 according as $m = p$ or $m \neq p$, and $\rho_h(\tau)$ is derived as follows and given by (7).

In flat Rayleigh fading channels, $h_{mn}(t)$, a zero-mean complex Gaussian random process, can be represented as [4]

$$h_{mn}(t) = h_{mn}^I(t) + \jmath h_{mn}^Q(t) = \alpha_{mn}(t)\exp[-\jmath\Phi_{mn}(t)], \tag{2}$$

where the zero-mean real Gaussian random processes $h_{mn}^I(t)$ and $h_{mn}^Q(t)$ are the real and imaginary parts of $h_{mn}(t)$, respectively. $\alpha_{mn}(t)$ is the envelope of $h_{mn}(t)$ and $\Phi_{mn}(t)$ is

[1]In this paper, each subchannel represents the radio link between each transmit/receive pair of antennas.

$$p(x,y)=\frac{e^{-(x+y)}}{4\varrho_i^2}\left\{\frac{\varrho_i^2-x+y(x-1)+1}{1-\varrho_i^2}\exp\left[-\frac{\varrho_i^2(x+y)}{1-\varrho_i^2}\right]I_0\left(\frac{2\varrho_i\sqrt{xy}}{1-\varrho_i^2}\right)-\left(y\varrho_i^2-\varrho_i^2-x+1\right)\left(x\varrho_i^2-\varrho_i^2-y+1\right)\right\},\quad x,y\geq 0. \tag{3}$$

$$\begin{aligned} r_{\mathcal{I}}(i)=&\frac{1}{\lambda_i^3\varrho_i^2}\sum_{k=0}^{\infty}\frac{\varrho_i^{2k}}{(k!)^2}\left\{\left[\lambda_i\varrho_i G_{2,3}^{3,1}\left(\frac{2\lambda_i}{\eta}\middle|\begin{matrix}0,1\\0,0,k+1\end{matrix}\right)\right]^2+\left[\lambda_i G_{2,3}^{3,1}\left(\frac{2\lambda_i}{\eta}\middle|\begin{matrix}0,1\\0,0,k+1\end{matrix}\right)-G_{2,3}^{3,1}\left(\frac{2\lambda_i}{\eta}\middle|\begin{matrix}0,1\\0,0,k+2\end{matrix}\right)\right]^2\right\}\\ &+2\left\{G_{2,3}^{3,1}\left(\frac{2}{\eta}\middle|\begin{matrix}0,1\\0,0,1\end{matrix}\right)G_{2,3}^{3,1}\left(\frac{2}{\eta}\middle|\begin{matrix}0,1\\0,0,3\end{matrix}\right)-\left[G_{2,3}^{3,1}\left(\frac{2}{\eta}\middle|\begin{matrix}0,1\\0,0,2\end{matrix}\right)\right]^2\right\}-\frac{1}{\lambda_i^2\varrho_i^2}\left[G_{2,3}^{3,1}\left(\frac{2}{\eta}\middle|\begin{matrix}0,1\\0,0,1\end{matrix}\right)-G_{2,3}^{3,1}\left(\frac{2}{\eta}\middle|\begin{matrix}0,1\\0,0,2\end{matrix}\right)\right]^2. \end{aligned} \tag{4}$$

$$\mathbb{E}[\mathcal{I}_l]=G_{2,3}^{3,1}\left(\frac{2}{\eta}\middle|\begin{matrix}0,1\\0,0,3\end{matrix}\right)-2G_{2,3}^{3,1}\left(\frac{2}{\eta}\middle|\begin{matrix}0,1\\0,0,2\end{matrix}\right)+2G_{2,3}^{3,1}\left(\frac{2}{\eta}\middle|\begin{matrix}0,1\\0,0,1\end{matrix}\right). \tag{5}$$

$$\begin{aligned} \mathbb{E}[\mathcal{I}_l^2]=&4e^{\frac{2}{\eta}}\left[\frac{1}{2}G_{3,4}^{4,0}\left(\frac{2}{\eta}\middle|\begin{matrix}3,3,3\\3,2,2,2\end{matrix}\right)-G_{3,4}^{4,0}\left(\frac{2}{\eta}\middle|\begin{matrix}2,2,2\\3,1,1,1\end{matrix}\right)+\frac{1}{2}G_{3,4}^{4,0}\left(\frac{2}{\eta}\middle|\begin{matrix}1,1,1\\3,0,0,0\end{matrix}\right)+G_{3,4}^{4,0}\left(\frac{2}{\eta}\middle|\begin{matrix}2,2,2\\2,1,1,1\end{matrix}\right)-G_{3,4}^{4,0}\left(\frac{2}{\eta}\middle|\begin{matrix}1,1,1\\2,0,0,0\end{matrix}\right)\right.\\ &\left.+G_{3,4}^{4,0}\left(\frac{2}{\eta}\middle|\begin{matrix}1,1,1\\1,0,0,0\end{matrix}\right)\right]+2\left\{G_{2,3}^{3,1}\left(\frac{2}{\eta}\middle|\begin{matrix}0,1\\0,0,1\end{matrix}\right)G_{2,3}^{3,1}\left(\frac{2}{\eta}\middle|\begin{matrix}0,1\\0,0,3\end{matrix}\right)-\left[G_{2,3}^{3,1}\left(\frac{2}{\eta}\middle|\begin{matrix}0,1\\0,0,2\end{matrix}\right)\right]^2\right\}. \end{aligned} \tag{6}$$

the phase of $h_{mn}(t)$. At any time t, $\alpha_{mn}(t)$ has a Rayleigh distribution and $\Phi_{mn}(t)$ is distributed uniformly over $[-\pi,\pi)$. Without loss of generality, we assume each subchannel has unit power, i.e., $\mathbb{E}[\alpha_{mn}^2(t)]=1$.

Using the empirically-verified [4] multiple von Mises probability density function (PDF) [9, (4)] for the angle of arrival (AoA) at the receiver in *non-isotropic* scattering environments shown as Fig. 1 [9], the channel correlation coefficient $\rho_h(\tau)$ of $h_{mn}(t)$, $\forall m,n$, is given by [9, (7)]

$$\begin{aligned} \rho_h(\tau)&=\mathbb{E}[h_{mn}(t)h_{mn}^*(t-\tau)],\\ &=\sum_{n=1}^{N}P_n\frac{I_0(\sqrt{\kappa_n^2-4\pi^2f_D^2\tau^2+j4\pi\kappa_n f_D\tau\cos\theta_n})}{I_0(\kappa_n)}, \end{aligned} \tag{7}$$

where $I_k(z)=\frac{1}{\pi}\int_0^{\pi}e^{z\cos\theta}\cos(k\theta)\mathrm{d}\theta$ is the k^{th} order modified Bessel function of the first kind. θ_n is the mean AoA of the n^{th} cluster of scatterers, κ_n controls the width of the n^{th} cluster of scatterers, P_n represents the contribution of the n^{th} cluster of scatterers, such that $\sum_{n=1}^{N}P_n=1, 0<P_n\leqslant 1$, N is the number of clusters of scatterers, and f_D is the maximum Doppler frequency. When $\kappa_n=0,\forall n$, which corresponds to the *isotropic* scattering, (7) reduces to $\rho_h(\tau)=I_0(j2\pi f_D\tau)=J_0(2\pi f_D\tau)$ [9].

Similar to the SISO systems considered in [6], we consider a piecewise constant approximation for the continuous-time fading channel coefficient $\mathbf{H}(t)$, represented by $\{\mathbf{H}(lT_s)\}_{l=1}^{L}$, where T_s is the symbol duration and L is the number of samples. In the presence of additive white Gaussian noise, if perfect channel state information $\{\mathbf{H}(lT_s)\}_{l=1}^{L}$, is available at the receiver only, the ergodic channel capacity is given by [7][12]

$$C=\mathbb{E}\left[\ln\det\left(\mathbf{I}_2+\frac{\eta}{2}\mathbf{H}_l\mathbf{H}_l^{\dagger}\right)\right], \tag{8}$$

nats/s/Hz, where η is the average SNR at the receiver side, and $\mathbf{H}_l$ denotes $\mathbf{H}(lT_s)$.

In the above equation, at any given time index l, $\ln\det\left(\mathbf{I}_2+\frac{\eta}{2}\mathbf{H}_l\mathbf{H}_l^{\dagger}\right)$ is a random variable as it depends on the fading parameter $\mathbf{H}_l$. Therefore

$$\mathcal{I}_l=\ln\det\left(\mathbf{I}_2+\frac{\eta}{2}\mathbf{H}_l\mathbf{H}_l^{\dagger}\right),\quad l=1,2,\cdots, \tag{9}$$

is a discrete-time random process with the ergodic capacity as its mean. We study the second-order statistics of $\{\mathcal{I}_l\}_{l=1}^{\infty}$, such as autocorrelation and correlation coefficient, in the following section.

III. ACF and Correlation Coefficient of MIMO IMI

In this section, first we concentrate on the ACF of MIMO IMI in (9), which is defined by

$$r_{\mathcal{I}}(i)=\mathbb{E}[\mathcal{I}_l\mathcal{I}_{l-i}], \tag{10}$$

$$=\mathbb{E}\left[\ln\det\left(\mathbf{I}_2+\frac{\eta}{2}\mathbf{H}_l\mathbf{H}_l^{\dagger}\right)\ln\det\left(\mathbf{I}_2+\frac{\eta}{2}\mathbf{H}_{l-i}\mathbf{H}_{l-i}^{\dagger}\right)\right]. \tag{11}$$

We assume x_1 and x_2 are two *unordered* eigenvalues of $\mathbf{H}_l\mathbf{H}_l^{\dagger}$, and y_1 and y_2 are two *unordered* eigenvalues of $\mathbf{H}_{l-i}\mathbf{H}_{l-i}^{\dagger}$. Moreover, x is *randomly* selected from x_1 and x_2, and y is *randomly* selected from y_1 and y_2. Therefore, (11) reduces to

$$\begin{aligned} r_{\mathcal{I}}(i)&=\mathbb{E}\left[\sum_{m=1}^{2}\ln\left(1+\frac{\eta}{2}x_m\right)\sum_{n=1}^{2}\ln\left(1+\frac{\eta}{2}y_n\right)\right],\\ &=4\mathbb{E}\left[\ln\left(1+\frac{\eta}{2}x\right)\ln\left(1+\frac{\eta}{2}y\right)\right]. \end{aligned} \tag{12}$$

To further simplify (12), we need the joint PDF of x and y, which is given by (3) [13], where $\varrho_i=|\rho_h(iT_s)|<1$, $i\neq 0$, $\rho_h(\tau)$ is presented in (7). The marginal PDF of x is given by

$$p(x)=\left(\frac{x^2}{2}-x+1\right)e^{-x}, x\geq 0, \tag{13}$$

by integrating (3) over the variable y, which is also given in [12].

Combination (3) and (12), with the following Taylor series of $I_0(t)$ [14, pp. 971, 8.447.1]

$$I_0(t)=\sum_{k=0}^{\infty}\frac{t^{2k}}{(k!)^2 2^{2k}}, \tag{14}$$

simplifies (10) to the exact infinite-summation closed-form representation in (4), where G is Meijer's G function [14, pp. 1096, 9.301] and

$$\lambda_i = \frac{1}{1-\varrho_i^2}. \tag{15}$$

With $\mathcal{I}_l = \sum_{m=1}^{2} \ln\left(1+\frac{\eta}{2}x_m\right)$, the first moment of $\mathcal{I}_l$ is shown to be (5), and the second moment of $\mathcal{I}_l$ is

$$\mathbb{E}\left[\mathcal{I}_l^2\right] = 2\mathbb{E}\left[\ln^2\left(1+\frac{\eta}{2}x_1\right) + \ln\left(1+\frac{\eta}{2}x_1\right)\ln\left(1+\frac{\eta}{2}x_2\right)\right], \tag{16}$$

which reduces to (6) by using the marginal PDF in (13) and the joint PDF of x_1 and x_2 [15, (2.22)]

$$p(x_1,x_2) = \frac{1}{2}\left(x_1-x_2\right)^2 e^{-(x_1+x_2)}, \quad x_1,x_2 \geq 0. \tag{17}$$

Therefore the normalized ACF and correlation coefficient can be calculated according to

$$\tilde{r}_{\mathcal{I}}(i) = \frac{r_{\mathcal{I}}(i)}{\mathbb{E}[\mathcal{I}_l^2]}, \tag{18}$$

and

$$\rho_{\mathcal{I}}(i) = \frac{r_{\mathcal{I}}(i) - \{\mathbb{E}[\mathcal{I}_l]\}^2}{\mathbb{E}[\mathcal{I}_l^2] - \{\mathbb{E}[\mathcal{I}_l]\}^2}, \tag{19}$$

by plugging (4) and (6) into (18), and (4)-(6) into (19), respectively.

In general, it seems difficult to further simplify (4). However, we note that the integral

$$\Xi(k,\omega,\lambda_i) = \int_0^\infty x^k e^{-\lambda_i x}\ln(1+\omega x)\mathrm{d}x, \quad k \geq 0, \tag{20}$$

can be approximated by

$$\Xi(k,\omega,\lambda_i) \approx \begin{cases} \int_0^\infty \omega x^{k+1} e^{-\lambda_i x}\mathrm{d}x, & \omega \to 0, \\ \int_0^\infty x^k e^{-\lambda_i x}\ln(\omega x)\mathrm{d}x, & \omega \to \infty, \end{cases} \tag{21}$$

using $\ln(1+\omega x) \approx \omega x$, $\omega \to 0$, and $\ln(1+\omega x) \approx \ln(\omega x)$, $\omega \to \infty$, respectively[2].

In the following two subsections, we obtain asymptotic closed-form expressions for the normalized ACF, $\tilde{r}_{\mathcal{I}}(i)$, and correlation coefficient, $\rho_{\mathcal{I}}(i)$, in low- and high-SNR regimes.

A. Low-SNR Regime

If $\eta \to 0$, based on (14) and (21), after some basic algebraic manipulations, we proved that the normalized ACF and the correlation coefficient are, respectively, expressed as

$$\tilde{r}_{\mathcal{I}}(i) \approx \frac{4+\varrho_i^2}{5}, \tag{22}$$

and

$$\rho_{\mathcal{I}}(i) \approx \varrho_i^2. \tag{23}$$

Interestingly, the above results are the same as those in the 2×2 MIMO with orthogonal space-time block code (OSTBC) transmission in low-SNR regimes, as expected. In fact, in low-SNR regimes, $\mathcal{I}_l$ in (9) can be approximated as $\mathcal{I}_l \approx \frac{\eta}{2}\|\mathbf{H}_l\|_F^2$, which is the same as the low-SNR approximation of $\mathcal{I}_l$ in MIMO-OSTBC systems [16].

With *isotropic* scattering, we have $\rho_h(iT_s) = J_0(2\pi f_D i T_s)$, the Clarke's correlation [1], this simplifies (23) to $J_0^2(2\pi f_D i T_s)$.

B. High-SNR Regime

If $\eta \to \infty$, based on (14) and (21), after lengthy algebraic calculations, we have shown that the normalized ACF and the correlation coefficient are, respectively, given by

$$\tilde{r}_{\mathcal{I}}(i) \approx \frac{2\,\mathrm{Li}_2\left(\varrho_i^2\right) - \varrho_i^2 + \left[2\ln\left(\frac{\eta}{2\gamma}\right)+1\right]^2}{\frac{\pi^2}{3} - 1 + \left[2\ln\left(\frac{\eta}{2\gamma}\right)+1\right]^2}, \tag{24}$$

and

$$\rho_{\mathcal{I}}(i) \approx \frac{2\,\mathrm{Li}_2\left(\varrho_i^2\right) - \varrho_i^2}{\frac{\pi^2}{3}-1}, \tag{25}$$

where $\gamma = 1.781072\cdots$ is the Euler-Mascheroni constant [14, pp. xxx], and $\mathrm{Li}_2(x)$ is the dilogarithm function, defined as

$$\mathrm{Li}_2(x) = \sum_{k=1}^{\infty}\frac{x^k}{k^2}, \quad |x| \leq 1. \tag{26}$$

With *isotropic* scattering, (25) reduces to

$$\rho_{\mathcal{I}}(i) \approx \frac{2\,\mathrm{Li}_2\left[J_0^2(2\pi f_D i T_s)\right] - J_0^2(2\pi f_D i T_s)}{\frac{\pi^2}{3}-1}. \tag{27}$$

IV. Numerical Results and Discussion

In this paper, the generalized power spectrum [9, (8)] is used to simulate Rayleigh flat fading channels with *non-isotropic* scattering, according to the spectral method [17]. To verify the accuracy of the derived formulas, we consider three types of scattering environments: *isotropic* scattering, *non-isotropic* scattering with three clusters of scatterers, and highly *non-isotropic* scattering with one cluster of scatterers ($\kappa = 40$, $\theta = \frac{10\pi}{9}$). For the *non-isotropic* scattering, parameters of three clusters, $[P_n, \kappa_n, \theta_n], n = 1,2,3$, are given by $[P_1,\kappa_1,\theta_1] = \left[0.45, 2, \frac{\pi}{18}\right]$, $[P_2,\kappa_2,\theta_2] = \left[0.2, 20, \frac{11\pi}{18}\right]$, and $[P_3,\kappa_3,\theta_3] = \left[0.35, 3, \frac{53\pi}{36}\right]$, respectively. In addition, in all the simulations, the maximum Doppler frequency f_D is set to 10Hz, and $T_s = \frac{1}{20 f_D}$ seconds.

In the following subsections, simulations are performed to verify the ACF and correlation coefficient of IMI in the above three types of environments in both low- and high-SNR regimes. For evaluating the approximation accuracy of ACF and the correlation coefficient, we set $\eta = -15$ dB for low SNR, and $\eta = 30$ dB for high SNR.

A. Isotropic Scattering

This is the Clarke's model, with uniform AoA. The simulation results are shown in Fig. 1.

B. Non-isotropic Scattering

This is a general case, with an arbitrary AoA distribution. Simulations are carried out, with the results presented in Fig. 2.

[2]The utility and accuracy of (21) is confirmed by Monte Carlo simulations in Sec. IV.

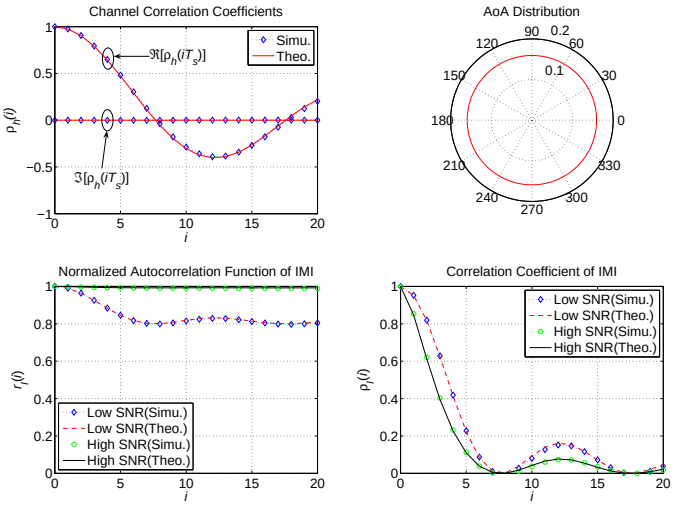

Fig. 1. The channel correlation coefficient, AoA distribution, as well as the normalized ACF and correlation coefficient of IMI, in a 2×2 MIMO system with *isotropic* scattering.

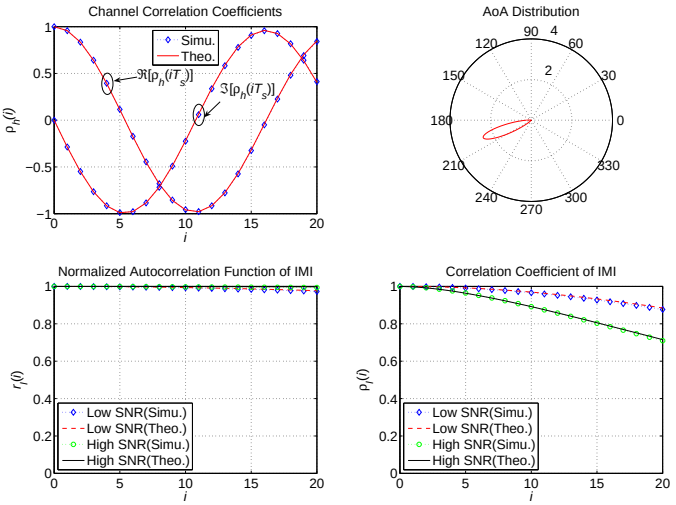

Fig. 3. The channel correlation coefficient, AoA distribution, as well as the normalized ACF and correlation coefficient of IMI, in a 2×2 MIMO system with highly *non-isotropic* scattering.

C. Highly Non-isotropic Scattering

This is a case where MS receive the signal within a very narrow beam. Simulation results are presented in Fig. 3.

In Figs. 1-3, The upper left and right figures show the channel correlation coefficient and AoA distributions; the lower left and right figures show the normalized approximate ACF and the approximate correlation coefficient of the IMI $\mathcal{I}_l$, respectively, in both low- and high-SNR regimes. In all figures, 'Simu." means simulation, and "Theo." means the channel coefficient $\rho_h(\tau)$, the normalized ACF and correlation coefficient in low- and high-SNR regimes are calculated according to (7), (22), (23), (24), and (25), respectively.

From Figs. 1-3, the following observations can be made.

- In both low- and high-SNR regimes, the asymptotic results of the normalized ACF and correlation coefficient derived in Sec. III perfectly match the simulation results in all the three scenarios we considered.
- The narrower of the angle spread at the receiver side, the larger the correlation coefficient. It implies that the instantaneous mutual information has less fluctuation when the receiver takes the signal from a narrow angle, which is the same as the results we obtained in the SISO systems [9].
- In all scenarios we considered, there are obvious gaps, which can not be ignored, between low- and high-SNR asymptotic approximations. Therefore, for not so small or large SNRs, we need to resort to the exact formulas in (4)-(6) for the accurate values of correlations. For example, $\eta = 15$dB, the simulation and theoretical curves, as well as low- and high-SNR approximations are shown in Fig. 4 for the correlation coefficient.

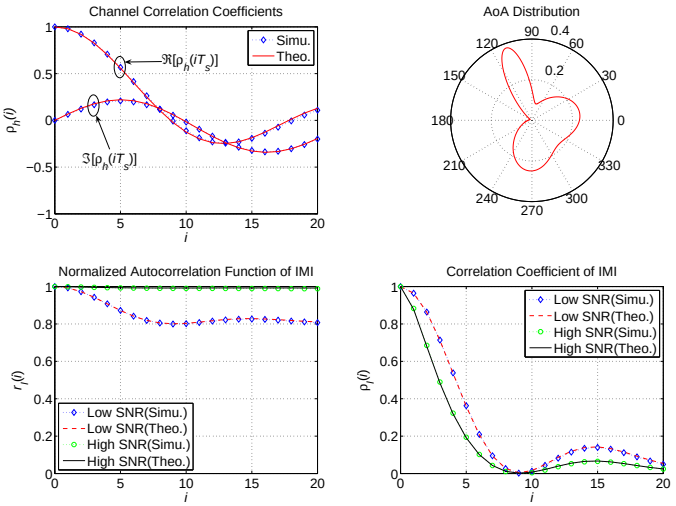

Fig. 2. The channel correlation coefficient, AoA distribution, as well as the normalized ACF and correlation coefficient of IMI, in a 2×2 MIMO system with *non-isotropic* scattering.

V. Conclusion

In this paper, closed-form expressions for the autocorrelation function and correlation coefficient of the instantaneous mutual information (IMI) in time-varying Rayleigh flat fading channels are derived, in 2×2 MIMO systems. The analytical expressions, supported by Monte Carlo simulations, provide useful qualitative and quantitative information regarding the fluctuations of IMI.

In this paper, we only considered 2×2 MIMO systems. It is our ongoing work to consider the spatially uncorrelated general MIMO system with $M \geq 2$ transmitters and $N \geq 2$ receivers, where all the subchannels are independent and identically distributed, with the same temporal correlation function.

References

[1] W. C. Jakes, Ed., *Microwave Mobile Communications*. New York: IEEE Press, 1994.

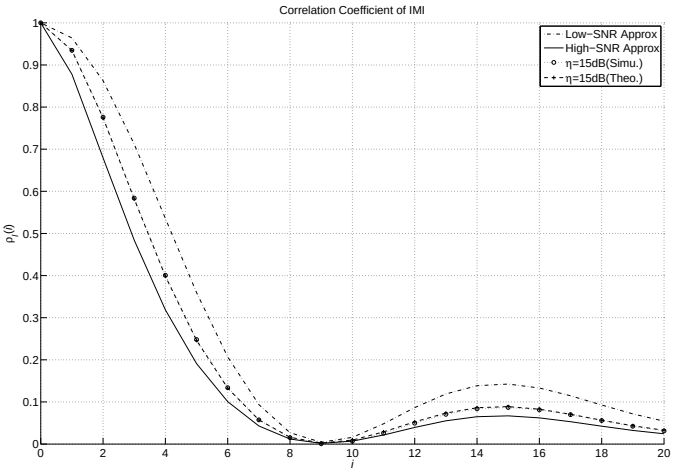

Fig. 4. The correlation coefficient of IMI at SNR $\eta = 15$dB, in a 2×2 MIMO system with *non-isotropic* scattering.

[2] A. Abdi, K. Wills, H. A. Barger, M. S. Alouini, and M. Kaveh, "Comparison of the level crossing rate and average fade duration of Rayleigh, Rice, and Nakagami fading models with mobile channel data," in *Proc. IEEE Veh. Technol. Conf.*, Boston, MA, 2000, pp. 1850–1857.

[3] N. Youssef, T. Munakata, and M. Takeda, "Fade statistics in Nakagami fading environments," in *Proc. IEEE Int. Symp. Spread Spec. Tech. App.*, Mainz, Germany, 1996, pp. 1244–1247.

[4] A. Abdi, J. A. Barger, and M. Kaveh, "A parametric model for the distribution of the angle of arrival and the associated correlation function and power spectrum at the mobile station," *IEEE Trans. Veh. Technol.*, vol. 51, pp. 425–434, May 2002.

[5] A. Abdi, W. C. Lau, M. S. Alouini, and M. Kaveh, "A new simple model for land mobile satellite channels: First- and second-order statistics," *IEEE Trans. Wireless Commun.*, vol. 2, pp. 519–528, May 2003.

[6] L. H. Ozarow, S. Shamai, and A. D. Wyner, "Information theoretic considerations for cellular mobile radio," *IEEE Trans. Veh. Technol.*, vol. 43, pp. 359–378, May 1994.

[7] D. Tse and P. Viswanath, *Fundamentals of Wireless Communication*. Cambridge, UK: Cambridge University Press, 2005.

[8] B. M. Hochwald, T. L. Marzetta, and V. Tarokh, "Multiple-antenna channel hardening and its implications for rate feedback and scheduling," *IEEE Trans. Inform. Theory*, vol. 50, pp. 1893–1909, 2004.

[9] S. Wang and A. Abdi, "On the second-order statistics of the instantaneous mutual information of time-varying fading channels," in *Proc. IEEE Int. Workshop Signal Processing Advances in Wireless Communications*, New York, 2005, pp. 405–409.

[10] A. Giorgetti, M. Chiani, M. Shafi, and P. J. Smith, "Level crossing rates and MIMO capacity fades: impacts of spatial/temporal channel correlation," in *Proc. IEEE Int. Conf. Commun.*, Anchorage, AK, 2003, pp. 3046–3050.

[11] N. Zhang and B. Vojcic, "Evaluating the temporal correlation of MIMO channel capacities," in *Proc. IEEE Global Telecommun. Conf.*, St. Louis, MO, 2005, pp. 2817–2821.

[12] İ. E. Telatar, "Capaicty of multi-antenna Gaussian channels," *European Trans. Telecommun.*, vol. 10, pp. 585–595, 1999.

[13] S. Wang and A. Abdi, "Joint singular value distribution of two correlated rectangular complex Gaussian matrices and its application," submitted, 2006.

[14] I. S. Gradshteyn, I. M. Ryzhik, and A. Jeffrey, Eds., *Table of Integrals, Series, and Products*, 5th ed. San Diego, CA: Academic, 1994.

[15] A. M. Tulino and S. Verdú, "Random matrices and wireless communications," *Foundations and Trends in Communications and Information Theory*, vol. 1, June 2004.

[16] S. Wang and A. Abdi, "On the second-order statistics of the instantaneous mutual information in Rayleigh fading channels," submitted, 2005.

[17] K. Acolatse and A. Abdi, "Efficient simulation of space-time correlated MIMO mobile fading channels," in *Proc. IEEE Veh. Technol. Conf.*, Orlando, FL, 2003, pp. 652–656.